Proceedings of ISAP'04, Sendai, JAPAN

STUDY OF HIGH GAIN AND BROADBAND ANTIPODAL FERMI ANTENNA WITH CORRUGATION

Yukiko TAKAGI, Hiroyasu SATO,
Yoshihiko WAGATSUMA†, Koji MIZUNO† and Kunio SAWAYA
Graduate School of Engineering, Tohoku University
Aza-Aoba 05, Aramaki, Aobaku, Sendai, 980-8579, Japan
† Research Institute of Electrical Communication, Tohoku University
2-1-1, Katahira, Aobaku, Sendai, 980-8577, Japan
E-mail: sahiro@ecei.tohoku.ac.jp

1. INTRODUCTION

Recently, there is a great demand for broadband antennas for the applications such as the ultra-wideband (UWB) communications, the EMI measurements and the wideband radars. Among many types of broadband antennas such as the bow-tie antenna, the log-periodic dipole array antenna, the spiral antenna, the TEM horn antenna and the double ridged horn antenna, the tapered slot antenna (TSA) is well known as a thin structure, low weight, easy to fabricate, well suited for microwave integrated circuits (MICs). In order to maintain the broadband characteristics of the TSA, it is important to design the TSA geometry including the taper profile and the balun section for a feeding line to slot line transition. Several taper profiles such as the LTSA (linearly TSA), the CWSA (constant width slot antenna) and the BLTSA (broken linearly TSA) have been proposed so far [1]. Also several baluns of MSL-slot transition [1], CPW-slot transition [2], [3] have been discussed. The antipodal TSA [4], which directly transforms the MSL to the taper section without using the stub has been proposed.

Recently, Sugawara et al. have proposed a TSA called "FERMI antenna" [5] having a profile defined by the Fermi-Dirac function as well as the corrugation on the side of the substrate. In our previous paper [6], a design of the FERMI antenna for passive millimeter wave (PMMW) imaging has been performed and the relation between the parameters of the FERMI antenna and the radiation pattern has been investigated by using the FDTD analysis.

In this paper, the antipodal FERMI antenna (APFA) with the combination of antipodal feeding section and FERMI taper section is proposed. A design of the high gain APFA by employing the corrugation is presented for broadband operation.

2. NUMERICAL AND EXPERIMENTAL INVESTIGATIONS

Fig. 1 shows the geometry of the APFA. The Fermi-Dirac taper is determined by $f(x) = a/(1+e^{-b(x-c)})$ where a denotes the asymptotic value of the width of the taper for $x \to \infty$ and c denotes the x coordinate of the inflection point of the Fermi-Dirac function. Because of the relation of $f'(c) = ab/4$, b is related to the gradient at the inflection point c. Also there is a relation of $f(c) = a/2$ and $W = 2a$ when $b(L-c) \gg 1$.

Table 1 shows the parameters of the APFA used in the present design. The FDTD analysis and the measurement were performed in the frequency range of 2GHz to 18GHz. In the numerical analysis, the cell size is Δx=0.4mm, Δy=0.2mm and Δz=0.25mm, respectively. The number of time steps was 30,000 and the 8-layer PML was used. The antenna is separated $40\Delta x$, $42\Delta y$ and $68\Delta z$ from the PML in each direction. A gaussian pulse was used for the excitation of the MSL and the delta gap feed was used with 50 Ω internal resistance.

The measurement of the actual gain was performed using 4 standard gain horn antennas with different frequency bands (3.94 - 5.99GHz, 5.38 - 8.18GHz, 8.20 - 12.5GHz, 11.9 - 18.0GHz).

3. RESULTS

In order to evaluate the balun section for the transition from the MSL to the parallel line, S-parameters of the tapered balun with back-to-back configuration were measured and are shown in Fig. 2. It is observed that the return loss is greater than 10dB in the frequency range of 2GHz

ISBN: 4-88552-206-4 C3055©IEICE

to 13.5GHz. Small insertion loss is also obtained in the broadband frequency range, however, the increase of insertion loss is observed as the frequency increases.

The VSWR of the APFA is shown in Fig. 3. It is observed that the calculated VSWR almost agree with the measured data and VSWR$\leq$2 is obtained in the frequency range of 5.8GHz to 14.4GHz (1:2.5).

The actual gain of the APFA with and without the corrugation is shown in Fig. 4. Discontinuities of the curves for the measured data are observed due to the difference of standard horn antennas but the maximum value of the difference is less than 0.3dB. The calculated values are higher than the measured values which might be caused by the copper loss and dielectric loss which are not considered in the FDTD analysis. The gain for the case with the corrugation is higher than the case without the corrugation in the broadband frequency range. The values of measured actual gain in the case with and without the corrugation at 10GHz were 13.3dBi and 10.2dBi, respectively. However, the gains for both cases decrease in the higher frequency region which might be caused by the insertion loss of the tapered balun.

Fig. 5 shows the radiation patterns of the APFA at 10GHz. Good agreement between the measured and the calculated values is observed in both E-plane and H-plane. Axially asymmetric sidelobe in the E-plane is observed which is caused by the asymmetric geometry of antipodal taper section, however, the low sidelobe levels of -19.3dB and -19.5dB in E-lane and H-plane are obtained.

The cross polarization level of the APFA with and without the corrugation is shown in Fig. 6. In the case without the corrugation, the measured cross polarization levels of E-plane and H-plane are less than -10dB in the frequency range of 4GHz to 16GHz. On the other hand, the measured cross polarization levels are less than -15dB for 4GHz to 16GHz in the case with the corrugation and an improvement of around 5dB is observed. The calculated results also show lower cross polarization by the presence of the corrugation.

Fig. 7 shows the actual gain of the APFA with changing the position of the inflection point c. In the case when $c = \lambda_0$, the higher gain is observed in the broadband frequency range than the case of $c = 2\lambda_0$ for both the FDTD analysis and the experiment. The values of measured actual gain in the case of $c = \lambda_0$ at 10GHz is 14.1dBi. This can be considered that the effective length of antenna for the case of c=λ_0 is longer than that for the case of c=$2\lambda_0$.

4. CONCLUSION

A antipodal FERMI antenna with corrugation has been proposed. A broadband characteristics of about 1:2.5, high gain and the lower cross polarization level of E-plane and H-plane have been obtained by the presence of the corrugation. It has been also found that the higher gain is obtained in the broadband frequency range by placing the position of the inflection point near the feeding point.

REFERENCES

[1] R. Q. Lee and R. N. Simons, "Advances in Microstrip and Printed Antennas," H. F. Lee and W. Chen ed., ch. 9, John Willy & Sons Inc., 1997.

[2] T. Q. Ho and S. M. Hart, "A Broad-Band Coplanar Waveguide to Slotline Transition," IEEE Microwave and Guided Wave Letters, Vol. 2, No. 10, pp. 415–416, 1992.

[3] K. P. Ma, Y. Qian, T. Itoh, "Analysis and Applications of a New CPW-Slotline Transition," IEEE Transactions on Microwave Theory and Techniques, Vol. 47, No. 4, 1999.

[4] E. Gazit, "Improved design of the Vivaldi antenna," IEE proc. H, Vol. 135, No. 2, pp. 89-92, 1988.

[5] S. Sugawara, Y. Maita, K. Adachi, K. Mori and K. Mizuno, "A mm-wave tapered slot antenna with improved radiation pattern," IEEE MTT-S International Microwave Symposium Digest, pp. 959–962, Denver, USA, 1997.

[6] H. Sato, N. Arai, Y. Wagatsuma, K. Sawaya and K. Mizuno, "Design of Millimeter Wave Fermi Antenna with Corrugation," IEICE Trans. (B), Vol. J86-B, No. 9, pp. 1851–1859, 2003 (in Japanese).

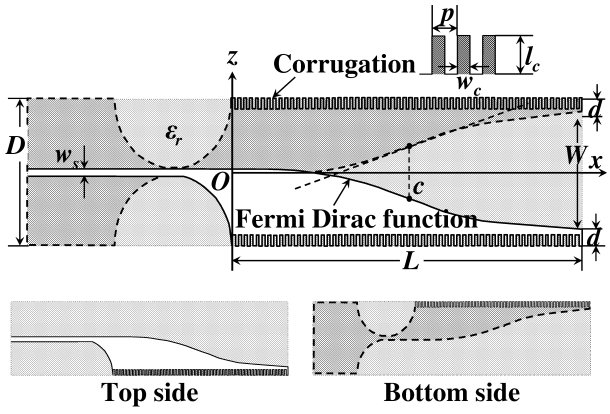

Figure 1: Geometry of APFA with corrugation.

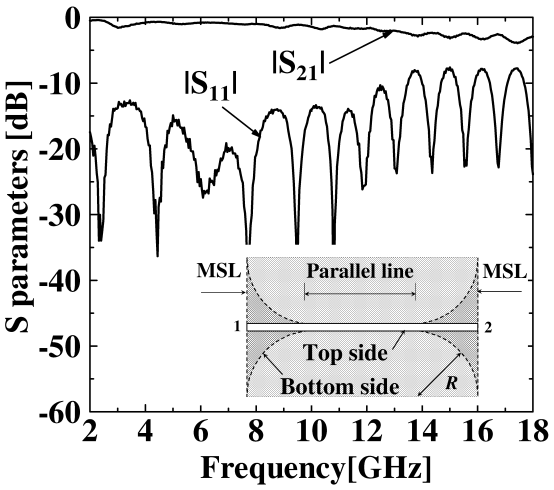

Figure 2: Measured S-parameters of back-to-back tapered balun, R=20mm.

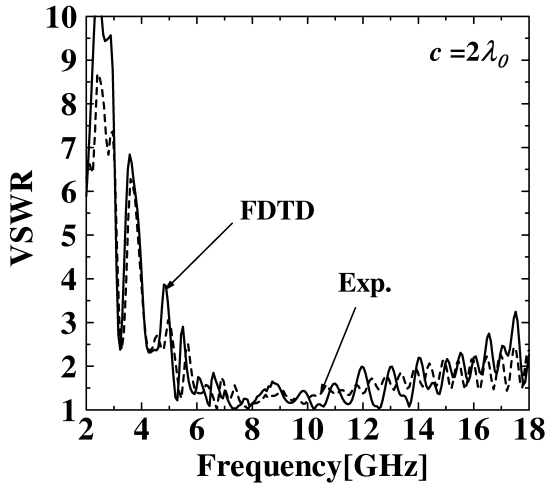

Figure 3: VSWR of APFA with corrugation.

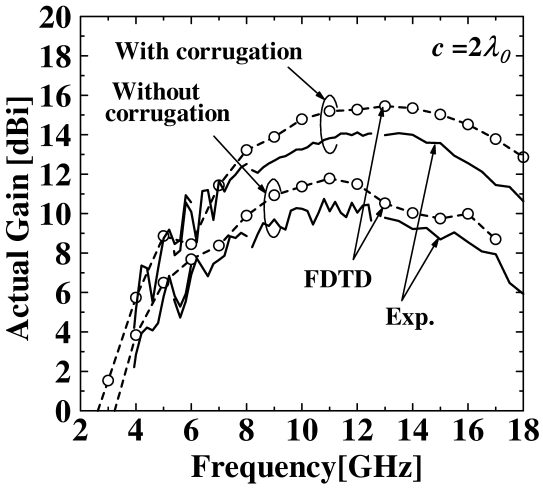

Figure 4: Actual gain of APFA with and without corrugation.

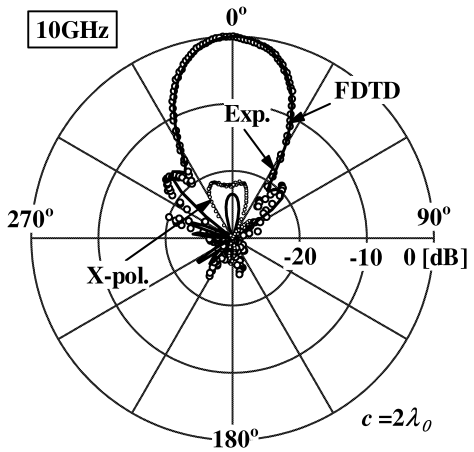

(a) E-plane

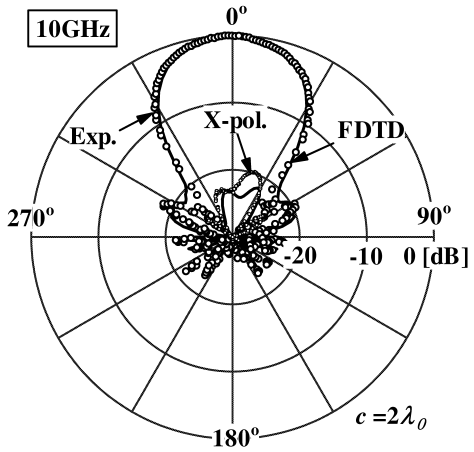

(b) H-plane

Figure 5: Radiation pattern of APFA with corrugation at 10 GHz.

Table 1: Parameters of APFA.

Dimensions	[mm]	[λ_0]@10GHz	Number of cells
Length of antenna L	120	4	$300\Delta x$
Width of aperture W	30	1	$120\Delta z$
Distance between the edges of aperture and substrate d	6	0.2	$24\Delta z$
Width of substrate D	42	1.4	$168\Delta z$
Thickness of substrate h	0.8	0.027	$4\Delta y$
Length of corrugation l_c	5	0.167	$20\Delta z$
Width of corrugation w_c	0.8	0.027	$2\Delta x$
Pitch of corrugation p	1.6	0.056	$4\Delta x$
Width of Slot line w_s	2	0.067	$8\Delta z$

a=15mm, b=2.4/λ_0, $2a = W$, $f(c) = a/2$

Δx=0.4mm, Δy=0.2mm, Δz=0.25mm, ε_r=3.3

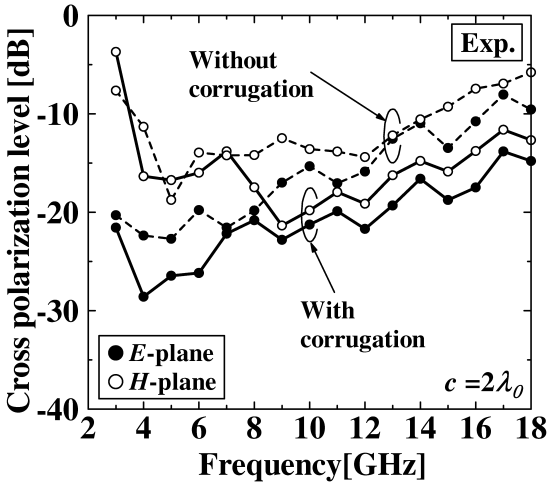

(a) Experiment

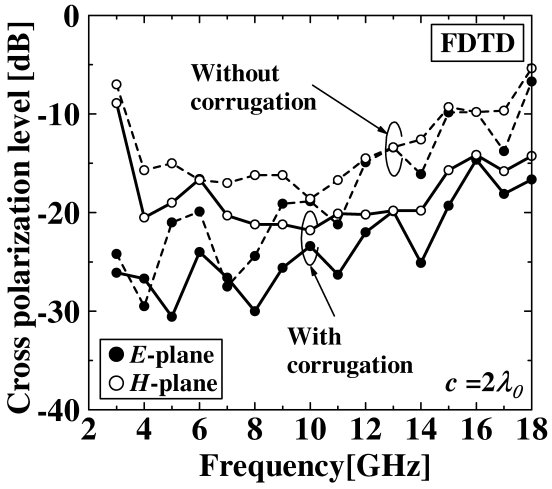

(b) FDTD

Figure 6: Cross polarization level of APFA with and without corrugation.

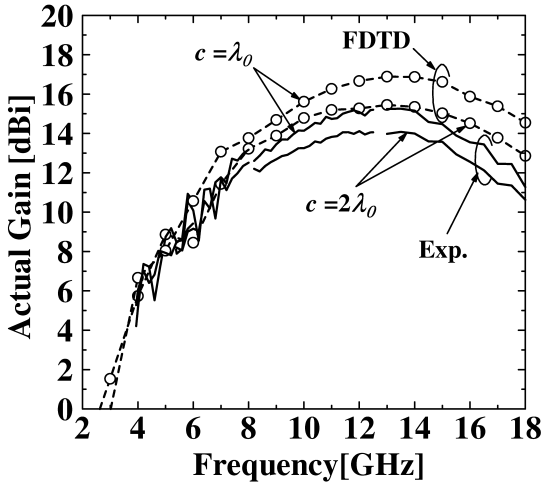

Figure 7: Actual gain of APFA with changing inflection point.